Vibrational Spectroscopy 62 (2012) 258–263

Contents lists available at SciVerse ScienceDirect

Vibrational Spectroscopy

journal homepage: www.elsevier.com/locate/vibspec

Raman scattering study of temperature induced phase transitions in crystalline ammonium heptafluorozirconate, $(NH_4)_3ZrF_7$

A.S. Krylov [a], S.N. Krylova [a,*], N.M. Laptash [b], A.N. Vtyurin [a]

[a] L. V. Kirensky Institute of Physics, Krasnoyarsk 660036, Russia
[b] Institute of Chemistry, 690022 Vladivostok, Russia

ARTICLE INFO

Article history:
Received 29 March 2012
Received in revised form 3 July 2012
Accepted 5 July 2012
Available online 16 July 2012

Keywords:
Raman spectroscopy
Phase transition
Ammonium heptafluorozirconate
Low temperature

ABSTRACT

This paper reports on a Raman spectroscopy investigation of phase transitions in $(NH_4)_3ZrF_7$ crystal. Raman spectra were obtained and analyzed in a wavenumber range from 3800 to 15 cm^{-1} and in the temperature range from 7 to 360 K. The anomalies caused by a series of subsequent structural phase transitions have been analyzed. A soft phonon mode restoring in the distorted phase was found. The spectral changes observed in the current study are similar to those typically found in phase transitions near a tricritical point. The spectral changes in the middle wavenumber range, 700–150 cm^{-1}, indicate that the phase transitions are due to structural ordering of pentagonal ZrF_7^{3-} bipyramids. Spectral data also show that a phase transition near 225 K is accompanied by an increase of the unit cell volume. In addition, spectral changes in the range of internal vibrations of ammonium ions indicate that the ion's motion slows down with decrease of temperature.

1. Introduction

Crystalline $(NH_4)_3ZrF_7$ attracts a special interest of the investigators. Ammonium heptafluorozirconate can be used as precursor for producing various functional materials like fluoride glasses [1] and water resistant textile coating [2], and for treatment of mineral ores [3].

Ammonium heptafluorozirconate (IV), $(NH_4)_3ZrF_7$, was first synthesized as early as in 1860 by Marignac [4]. In a century and a half since this discovery there have been a number of studies of its crystalline structure [5–10]. Different investigators agree that pentagonal bipyramid ZrF_7^{3-} groups in this crystal lattice are disordered at room temperature. It was also reported that the crystals decompose under normal pressure at temperatures above 580 K [11]. However, details of the crystal structure of the high temperature phase as well as the mechanism of phase transitions observed during cooling still remain unclear.

Experimental data regarding the high temperature phase of this crystal are controversial. For instance, Udovenko and Laptash [9] reported that the crystal structure of this compound corresponds to non-centrosymmetrical space group $F23$ (T^2), $Z=4$, with one of three crystallographically independent ammonium groups arranged in 6 or 12 equivalent orientations. However, according to other data [8,10], at room temperature, $(NH_4)_3ZrF_7$ crystallizes in centrosymmetrical space group, $Fm3m$ (O_h^5), $Z=4$, with two independent tetrahedral ammonium groups dynamically disordered.

NMR and X-ray studies showed that decrease of temperature down to 235–213 K causes structural transition of the crystal from cubic to rhombic phase [12,13]. Another study was carried out by utilizing polarization-optical method and X-ray spectroscopy [10]. This study found existence of a complex sequence of phases: cubic (G_1), rhombic (G_2), monoclinic (G_3), triclinic (G_4), and monoclinic (G_5), all observed in a temperature range from 280 down to 238 K. It was also reported that G_2, G_3, and G_4 transitions exhibited temperature hysteresis.

Yet another experimental technique frequently employed for investigation of phase transitions in crystals is vibrational spectroscopy. For example, phase transitions in fluoride compounds with elpasolite structure have been studied using vibrational spectroscopy [14–16]. Another example is the vibrational spectroscopy study of phase transitions in fluorides of main subgroup elements (ReF_7, IF_7), which have a crystalline structure of heptacoordinated complexes arranged into pentagonal bipyramids [17,18]. Infrared spectra and assignments have been reported for $(NH_4)_3ZrF_7$ and other fluorozirconates in the 4000–200 cm^{-1} region [19]. Given the well confirmed usefulness of Raman spectroscopy for investigation of phase transitions, we decided to utilize it in the current investigation of crystalline $(NH_4)_3ZrF_7$. According to Misyul et al. [10], transition from G_1 to G_2 is a second order phase transition, while transition from G_2 to G_3 is a first order phase transition. Phase transitions could be due to ordering of tetrahedral NH_4^+ as well as due

* Corresponding author.
E-mail address: slanky@iph.krasn.ru (S.N. Krylova).

0924-2031/$ – see front matter © 2012 Elsevier B.V. All rights reserved.
http://dx.doi.org/10.1016/j.vibspec.2012.07.003

to ordering of ZrF_7^{3-} pentagonal bipyramids. It is known [20] that a second order phase transition could be accompanied by condensation of the optical phonon which in this case should be observed in the Raman spectrum of the low symmetry phase. In the current study we concentrated our efforts on the search for such vibrations in the Raman spectra of $(NH_4)_3ZrF_7$.

2. Experimental methods and data processing

We used non-oriented microcrystals with average size about 200 μm obtained from the same crystallization as described in [10]. Raman spectra were collected in a backscattering geometry, using a triple-monochromator Jobin Yvon T64000 Raman spectrometer operating in double subtractive mode, and then detected by a charge-coupled device cooled at 140 K. The spectral resolution for the recorded Stokes side Raman spectra was set to ~1 cm^{-1} (this resolution was achieved by using gratings with 1800 grooves mm^{-1} and 100 μm slits). Single-mode argon 514.5 nm line from a Spectra-Physics Stabilite 2017 Ar+ laser of 100 mW power (20 mW on the sample) was used as excitation light source. The intensity of the laser light was adjusted to avoid sample heating. A closed cycle helium cryostat, ARS CS204-X1.SS, was utilized for temperature studies. This equipment ensures that the sample temperature during recording of the spectra is stabilized to within 0.05 K. Raman spectra were recorded in the temperature range from 7 to 360 K.

Positions and widths of spectral lines with maxima $\omega > 100\ cm^{-1}$ were obtained by least square fitting of the experimental data to the Lorentzian equation [21]:

$$I_L(x) = \frac{2}{\pi}\frac{A\Gamma}{4(x-\omega)^2+\Gamma^2}, \quad (1)$$

where A – amplitude, ω – wavenumber, Γ – full width at half height, and x – actual coordinate (wavenumber). The shape of the spectral lines with $\omega < 100\ cm^{-1}$ was described by equation of dumped harmonic oscillator [22]:

$$I_{DHO}(x) = F(\omega,T)\frac{2A\omega^2\Gamma x}{(\omega^2-x^2)^2+4\Gamma^2x^2}, \quad (2)$$

$$F(\omega,T) = \begin{cases} n(\omega)+1, & \omega > 0 \\ n(\omega), & \omega < 0 \end{cases} \quad (3)$$

$$n(\omega) = \left(\exp\left(\frac{c\hbar\omega}{k_BT}\right)-1\right)^{-1}, \quad (4)$$

where A – amplitude, ω – harmonic wavenumber (cm^{-1}), Γ – full width at half height, x – actual coordinate (wavenumber, cm^{-1}), c – speed of light, $\hbar$ – reduced Plank constant, and k_B – Boltzmann constant. Note that for spectral lines with ω greater than 100 cm^{-1}, the spectral parameters obtained by fitting these two shapes are in agreement to within experimental uncertainty.

3. Experimental results and discussion

To assist with spectral assignment we should note that the spectral lines in the low wavenumber range, e.g. below 150 cm^{-1}, correspond to lattice vibrations. The spectral lines in the range from 150 to 700 cm^{-1} correspond to internal vibrations of the ZrF_7^{3-} group, while the vibrations in the 1300–3800 cm^{-1} range are due to internal vibrations of ammonium ions.

Transformation of the Raman spectra of lattice vibrations with temperature in the wavenumber range below 150 cm^{-1} is shown in Fig. 1. Several new lines appear at temperatures below 240 K and become more pronounced as the temperature decreases. Arrows in Fig. 1 indicate two new lowest wavenumber features. Positions

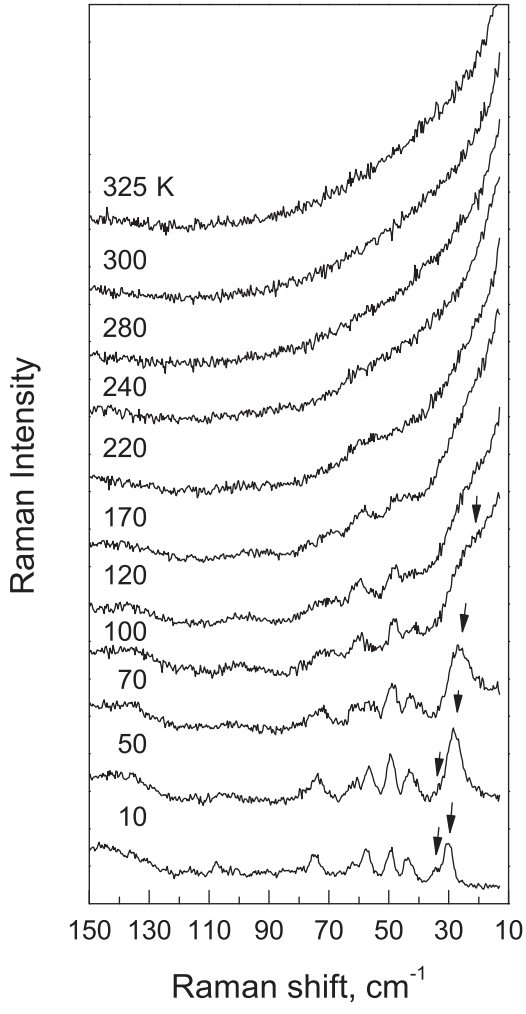

Fig. 1. Temperature transformation of Raman spectrum in the range 10–150 cm^{-1}.

of these low wavenumber features, 27 cm^{-1} and 35 cm^{-1}, respectively, at room temperature, shift with temperature as shown in Fig. 2. The insert in Fig. 2 shows the soft mode position ($\omega_s^2 = \omega^2 - \Gamma^2$) as a function of temperature (the lowest wavenumber feature). Good linear approximation, as evidenced by the insert

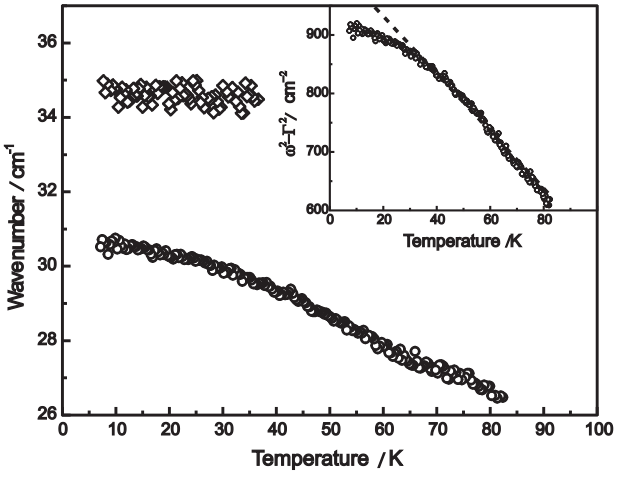

Fig. 2. Temperature dependencies of line positions in the range 20–40 cm^{-1}, the insert – wavenumber soft mode square $\omega^2 = \omega_0^2 - \Gamma^2$.

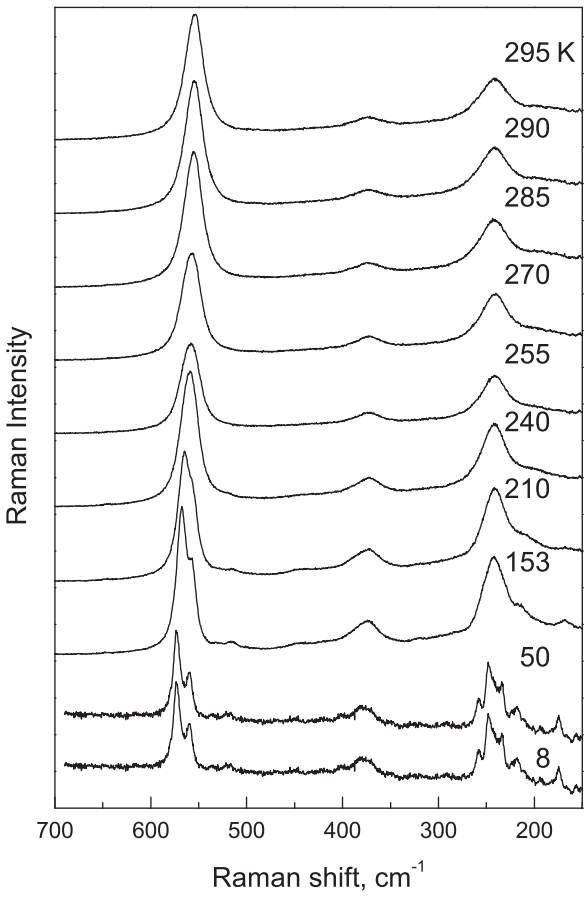

Fig. 3. Temperature transformation of Raman spectrum in the range 150–700 cm^{-1}.

in Fig. 2, is typical for soft modes corresponding to phase transitions near tricritical points [20].

Transformation of the Raman spectrum in the wavenumber range associated with vibrations of the ZrF_7^{3-} group is shown in Fig. 3. We can see only 3 Raman lines in this range (Fig. 3) and may be one more very week line near 205 cm^{-1}, but we cannot define its position clearly. At higher temperatures spectra were recorded over smaller temperature intervals. This was done to improve resolutions since as many as five phase transitions have been previously observed [10] during cooling of the samples down to 238 K. However, in this study we found the most pronounce changes at temperature below 240 K.

The experimental vibrational modes of ZrF_7^{3-} obtained in this study are given in Table 1 along with the results of theoretical calculations [23,24] carried out for C_{2v} and D_{5h} geometries.

The totally symmetrical mode is underlined. One can see that the calculated number of spectral lines as well as their positions for ZrF_7^{3-} (D_{5h}) complex agree better with the experimental observations. The correlation diagram of vibrational modes of ZrF_7^{3-} for C_{2v} and D_{5h} geometries is shown in Fig. 4. We expected 5 Raman lines for the D_{5h} symmetry and 18 lines for the C_{2v} symmetry for an isolated ZrF_7^{3-} ion (Fig. 4). Unfortunately we can see only 3 peaks.

The D_{5h} symmetry group of the free ion is not a subgroup of the O_h factor group of the crystal; that supposes the pentagonal bipyramidal ZrF_7^{3-} groups to be disordered in this crystal lattice, and a complete factor group analysis is not valid for them. Correlation diagrams for C_{2v} and O_h groups are presented in supplementary materials. According to Ref. [9], the structure of $(NH_4)_3ZrF_7$ corresponds to *F*23 symmetry (point group *T*). In this case the local symmetry of ZrF_7^{3-} ions can be only C_3 that give rise to 12 Raman active modes [17] – too many to agree with the 3 peaks found

Table 1
Normal vibrational modes of ZrF_7^{3-} group.

Symmetry species under C_{2v}			Symmetry species under D_{5h}						
Infrar. active	Raman active	Wavenum. (calcul.) [23], cm^{-1} ZrF_7^{3-}	Wavenum. (experim.) this work, $(NH_4)_3ZrF_7$ 300 K, cm^{-1}	Infrar. active	Raman active	Mode description [24]	Wavenum. (calcul.) ZrF_7^{3-} [23], cm^{-1}	Wavenum. (experim.) K_3ZrF_7 [25] 298 K, cm^{-1}	Wavenum. (experim.) Cs_3ZrF_7 [25] 298 K, cm^{-1}
A_1	A_1	299	240		E_1 //	δ rock XF_2 ax	217	247	234
A_1	A_1	466			A_1 /	ν sym XF_5 eq			
A_1	A_1	492		E_1 /		δ sciss XF_2 ax	300		
A_1	A_1			E_1 /		δ as XF_5 in plane	505		
A_1	A_1			E_1 /		ν as XF_5 eq			
A_1	A_1			A_2 //		δ umbrella XF_5 eq	240		
B_1	B_1	382		A_2 //		ν as XF_2 ax	478		
B_1	B_1	484	380		E_2 /	ν as XF_5 eq	405	327	312
B_1	B_1				E_2 /	Mixture of δ sciss XF_5 in plane		385	374
B_1	B_1		555		A_1 /	ν sym XF_2 ax	561	544	533
B_1	B_1								
A_1	A_1	581							
B_2	B_2	380							
B_2	B_2	519							
B_2	B_2								
B_2	B_2								
	A_2								
	A_2								

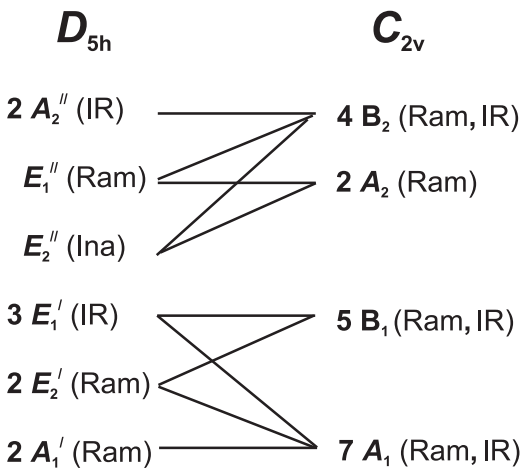

Fig. 4. Correlation diagram ZrF_7^{3-} vibrational modes for C_{2v} and D_{5h} local symmetries.

in the experimental spectra (Table 1). Therefore we assume the $(NH_4)_3ZrF_7$ crystal to be of O_h symmetry. The previously reported experimental data for K_3ZrF_7 and Cs_3ZrF_7 [25] are also given in Table 1 for comparison. Substitution of K^+ or Cs^+ ions by NH_4^+ leads to wavenumber increase of the totally symmetrical mode (Table 1).

Positions of vibrational modes vs. temperature in the range from 100 to 600 cm^{-1} are plotted in Fig. 5. As shown in Fig. 5, a new line near 173 cm^{-1} appears at 225 K and another one near 140 cm^{-1} appears at 210 K. We also observed appearance four other low-intensity lines below 170 K. Fig. 5 shows that at 225 K the spectral line near 562 cm^{-1} splits into 2 components. This spectral line corresponds to the stretching mode of the Zr—F bond (Table 1). Its temperature dependence deserves a detailed discussion.

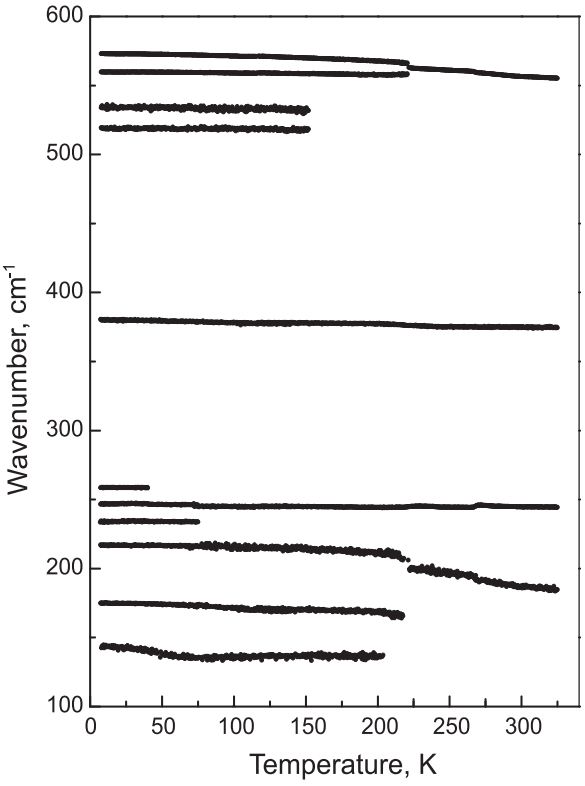

Fig. 5. Temperature dependencies of line positions in the range 100–600 cm^{-1}.

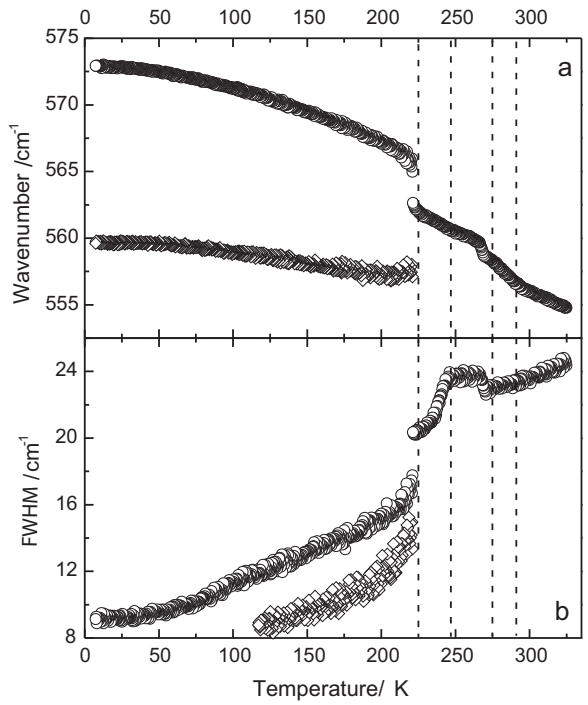

Fig. 6. Temperature dependencies of line positions (a) and full widths at half-maximum (b), detected in the range 550–575 cm^{-1}.

The wavenumber vs. temperature plot for this spectral line is given in Fig. 6a. The changes in the slope of this dependence are clearly seen at 291 K, 275 K, 247 K, and 225 K.

We assign these changes in the slope to structural phase transitions. The dashed vertical lines mark the transition temperatures. In addition, tentative assignment has been made for transitions at 266 and 238 K. Full width at half-maximum vs. temperature data for this spectral line are given in Fig. 6b. It was reported that in ordered non ammonium based elpasolite compounds such as Rb_2KScF_6 and Rb_2KInF_6, the linewidth (FWHM) of the Me-F stretching vibration of is about 10 cm^{-1} [11,13]. As shown in Fig. 5b, the linewidth of the νZr—F vibration of $(NH_4)_3ZrF_7$ is 24 cm^{-1} at 320 K which is far away from transition temperature. In other ammonium based elpasolites, such as $(NH_4)_3ScF_6$ and $(NH_4)_3GaF_6$, the linewidth of Me—F stretching vibration was reported to be about 20 cm^{-1} [26,27]. Authors argued that increase of linewidth of internal vibrations of ScF_6^{3-} is due to crystal disorder. It is known that significant increase of a linewidth could be due to anharmonicity as well as to disordering [28] of molecular ions [9,10]. In this particular case we believe that orientational disorder of ZrF_7^{3-} ions in the cubic phase crystals of ammonium fluorozirconate is the main factor contributing to the increase of the linewidth, in agreement with the data reported elsewhere [9,10,29]. Fig. 5b shows that during cooling there are no anomalous changes in the line width vs. temperature dependencies near the first phase transition at 291 K. This transition from cubic phase to a distorted phase appears to be smooth, which indicates that it might be a second order phase transition. Subsequent transitions do show sharp and significant changes in the linewidth vs. temperature dependency as can be clearly seen in Fig. 5b. Therefore, we believe that these subsequent phase transitions are accompanied by significant changes in the degree of ordering of pentagonal bipyramids. Additional cooling leads to significant reduction of the width of the stretching band; at 10 K it reduces to 9 cm^{-1} as can be seen in Fig. 5b. Since the stretching vibrational mode is totally symmetric, the appearance of a second line near 560 cm^{-1} at temperatures below 225 K is

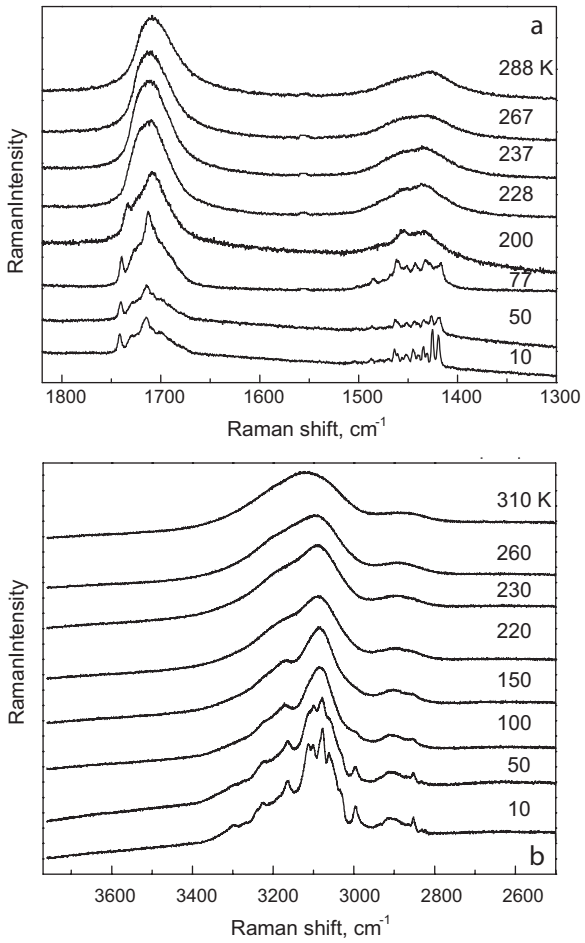

Fig. 7. Temperature transformation of Raman spectra of ammonium ions internal vibrations: (a) bending vibrations in the range 1350–1800 cm^{-1}, (b) stretching vibrations in the range 2600–3600 cm^{-1}.

probably due to increase (probably doubling) of the unit cell volume in the process of phase transition.

The normal modes of vibration of a free NH_4^+ ion under perfect T_d symmetry have wavenumbers of 3033, 1685, 3134, and 1397 cm^{-1} for ν_1 (A_1), ν_2 (E), ν_3 (F_2), and ν_4 (F_2) modes, respectively [30]. Raman bands due to ammonium groups are generally broad and it is difficult to distinguish between components. The bands at 1420 and 1715 cm^{-1} correspond to ν_4 and ν_2 bending vibrations, respectively, and the bands at 3100 and 2900 cm^{-1} are assigned to ν_3 and ν_1 stretching modes (see Fig. 7).

Transformation of Raman spectra in the wavenumber range 1800–1350 cm^{-1}, which is associated with internal bending vibrations of ammonium ions, is shown in Fig. 6a. Transformation of Raman spectra in a wavenumber range 3800–2600 cm^{-1}, which is associated with internal stretching vibrations of ammonium ions, is shown in Fig. 6b. Large, on the order of several hundred cm^{-1}, bandwidths for internal ammonium vibrations could be due to well known strong anharmonic effects in NH_4^+ ions [31] as well as due to orientational disordering of ammonium ions [8–10]. We expected the splitting of the doubly degenerate mode ν_2 (E) and the triply degenerated mode ν_3 (F_2) and ν_4 (F_2) in the low symmetry phases. Below the 225 K phase transition, the bandwidths in this spectral range reduced further and wide spectral bands evolve into complex multiline band shapes as indicated in Fig. 6a and b. These spectral changes could be explained by slowdown of motion of the ammonium ions below the phase transition temperature. This rationalization is in accordance with the previously reported data by Tarasov et al. [12] and Buslaev et al. [13].

4. Conclusions

Spectral anomalies observed in the Raman spectra of $(NH_4)_3ZrF_7$ crystals are due to phase transitions at $T_1 = 291$ K, $T_2 = 275$ K, $T_3 = 247$ K, and $T_4 = 225$ K. We also suppose that two other phase transitions occur at 266 K and 238 K, though evidence for these phase transitions is less conclusive. The most pronounced changes were found to be connected with vibrations of the ZrF_7^{3-} groups. The present study indicates that transition to the low temperature phase at $T_4 = 225$ K is accompanied by an increase of the unit cell volume. Transition from the cubic phase at $T_1 = 291$ K is gradual and thus presumed to be a second order transition. In the low wavenumber range recovery of a soft mode during sample cooling below 90 K were observed. Spectral changes with decrease of temperature were also observed in the region of the internal vibrations of the ammonium ions. Specifically, decrease of linewidths of internal vibrations below 225 K is suggested to be due to slower motion of ammonium ions at lower temperatures.

Acknowledgements

This work was partly supported by integration project SB RAS No 28, Russian Foundation for Basic Research project No 11-02-98002-r_siberia, No 12-02-00056, SS-4828.2012.2. The authors are grateful to Dr. I.N. Flerov for helpful discussions. The assistance of Dr. S. Skokov is sincerely appreciated.

Appendix A. Supplementary data

Supplementary data associated with this article can be found, in the online version, at http://dx.doi.org/10.1016/j.vibspec.2012.07.003.

References

[1] J.M. Parker, Annu. Rev. Mater. Sci. 19 (1989) 21–41.
[2] J.G. Hough, W.S. Rutherford, M. Smitt, Water resistant textile coating and method of using the same, United States Patent (1999) N 5874148.
[3] P.L. Crouse, W. Plessis, J.T. Nel, Book of Abstracts ISoFC, 2009, p. 105.
[4] C. Marignac, Ann. Chim. Phys. 60 (1860) 257–307.
[5] O. Hassel, H. Mark, Z. Phys. 27 (1924) 89–101.
[6] C.C. Hampson, Linus Pauling, J. Am. Chem. Soc. 60 (1938) 2702–2707.
[7] H.J. Hurst, J.C. Tailor, Acta Cryst. B 26 (1970) 417–421.
[8] H.J. Hurst, J.C. Tailor, Acta Cryst. B 26 (1970) 2136–2137.
[9] A.A. Udovenko, N.M. Laptash, J. Struct. Chem. 49 (2008) 482–488.
[10] S.V. Misyul, S.V. Mel'nikova, A.F. Bovina, N.M. Laptash, Phys. Solid State 50 (2008) 1951–1956.
[11] H.M. Haendler, C.M. Wheeler Jr., D.W. Robinson, J. Am. Chem. Soc. 74 (1952) 2352–2353.
[12] V.P. Tarasov, Yu.A. Buslaev, J. Struct. Chem. 10 (1969) 816–818.
[13] Yu.A. Buslaev, V.I. Pakhomov, V.P. Tarasov, V.N. Zege, Phys. Status Solidi B 44 (1971) K13–K15.
[14] S.N. Krylova, A.N. Vtyurin, A. Bulou, A.S. Krylov, N.G. Zamkova, Phys. Solid State 46 (2004) 1311–1319.
[15] A.S. Krylov, A. Bulou, S.N. Krylova, V.N. Voronov, A.N. Vtyurin, N.G. Zamkova, Comp. Mater. Sci. 36 (2006) 221–224.
[16] A.S. Krylov, S.N. Krylova, A.N. Vtyurin, N.V. Surovtsev, S.V. Adishev, V.N. Voronov, A.S. Oreshonkov, Crystallogr. Rep. 56 (2011) 18–23.
[17] H.H. Claassen, E.L. Gasner, H. Selig, J. Chem. Phys. 49 (1968) 1803–1807.
[18] H.H. Eysel, K. Seppelt, J. Chem. Phys. 56 (1972) 5081–5086.
[19] P.W. Smith, R. Stoessiger, A.G. Turnbull, J. Chem. Soc. A (1968) 3013–3015.
[20] J.F. Scott, Rev. Mod. Phys. 46 (1974) 83–128.
[21] V.K. Malinovsky, A.M. Pugachev, N.V. Surovtsev, Phys. Solid State 50 (2008) 1137–1143.
[22] L.H. Hoang, N.T.M. Hien, W.S. Choi, Y.S. Lee, K. Taniguchi, T. Arima, S. Yoon, X.B. Chen, In-Sang Yang, J. Raman Spectrosc. 41 (2010) 1005–1010.
[23] A.V. Voit, E.I. Voit, V.I. Sergienko, J. Struct. Chem. 40 (1999) 838–842.
[24] K.O. Christe, E.C. Curtis, D.A. Dixon, J. Am. Chem. Soc. 115 (1993) 1520–1526.
[25] V. Dracopoulos, J. Vagelatos, G.N. Papatheodorou, J. Chem. Soc., Dalton Trans. 7 (2001) 1117–1122.

[26] A.N. Vtyurin, A. Bulou, A.S. Krylov, M.L. Afanas'ev, A.P. Shebanin, Phys. Solid State 43 (2001) 2307–2310.
[27] M.L. Afanasiev, A.N. Vtyurin, S.V. Goryainov, A.S. Krylov, Bull. Russ. Acad. Sci. Phys. 68 (2004) 1072–1076.
[28] C. Carabatos-Nedelec, P. Becker, J. Raman Spectrosc. 28 (1997) 663–671.
[29] V.Ya. Kavun, I.A. Tkacenko, N.A. Didenko, V.I. Sergienko, J. Struct. Chem. 49 (2008) 1042–1047.
[30] K. Nakamoto, Infrared and Raman Spectra of Inorganic and Coordination Compounds, Part 2, 4th ed., John Wiley and Sons, New York, 1986, pp. 130–131.
[31] T.E. Jenkins, J. Phys. Condens. Matter. 19 (1986) 1065–1070.